Technology in Cancer Research and Treatment
ISSN 1533-0346
Volume 10, Number 1, February 2011

Dynamic Contrast Enhanced Optical Imaging of Capillary Leakage

www.tcrt.org

N. Faye, M.D.*
L. Fournier, M.D., Ph.D.
D. Balvay, Ph.D.
F. Taillieu, M.D.
C-A. Cuenod, M.D., Ph.D.
N. Siauve, M.D., Ph.D.
O. Clément, M.D., Ph.D.

Laboratory Research Imaging
Paris Cardiovascular Research Center
Inserm U970 56 rue Leblanc
75015 Paris, France
Université Paris Descartes UMR-S970,
Paris, France

We studied *in vivo* the vascular permeability of two fluorescent contrast agents in three types of capillary, using a fibered confocal fluorescence microscopy system.
Mice were imaged after injection of a macromolecular (albumin FITC 68,000 daltons) or low-molecular-weight contrast agent (FITC 389 daltons).
We studied continuous capillaries in muscles (FITC n = 4, albumin FITC n = 6), fenestrated capillaries in mesenteries (FITC n = 8, albumin FITC n = 10), and discontinuous capillaries in xenografted tumors (FITC n = 2, albumin FITC n = 4). Signal intensity (SI) was measured in capillary and interstitial regions, and time-enhancement curves were drawn. Two-compartment models were constructed to determine quantitative microcirculation parameters.
The arrival of the bolus of the two different contrast agents was observed in mesentery and muscle capillaries but not in tumor capillaries. Interstitial leakage of the low-molecular-weight contrast agent was observed almost instantaneously, whereas the macromolecular agent remained within the vessels. Signal intensity declined over the observation period, specifically in the tumor. No quantitative microcirculation parameters could be obtained with either of two bi compartmental models, owing to model instability.
This study shows that the microcirculation can be reproducibly observed in different types of capillary *in vivo* with this fibered fluorescence imaging device. Further work is required to quantify microvascular parameters.

Key words: Videomicroscopy; Optical imaging; Microcirculation; FITC; Albumin FITC.

Introduction

The microcirculation (1) is essential for tissue homeostasis and metabolism. It is regulated by tissue requirements and ensures fluid and solute exchanges at the microscopic level. These exchanges depend on the type of capillary and the nature of the endothelial wall. Transcapillary exchanges are also important for tumor growth, and tumor vessel wall abnormalities may play a role in tumor development and metastasis (2). New imaging methods are needed to study tumor microcirculation and angiogenesis, and for the evaluation of new antiangiogenic drugs (3).

Three types of blood capillary were described in the early 1950s, based on electron microscopy (4). The most frequent type in humans is the continuous capillary, which has a continuous basement membrane and tight junctions between epithelial cells, and is found in muscle and lung tissue. Molecules larger than 5 kDa are unable to pass through the endothelial wall. Fenestrated capillaries have pores approximately 70 nm in diameter, allowing smaller molecules to pass into the interstitium, but not larger molecules such as albumin.

Corresponding author:
Nathalie Faye, M.D.
E-mail: nath.faye@hotmail.fr

They are found in the mesentery, kidneys and endocrine glands. Discontinuous sinusoidal capillaries have a discontinuous or non existent basement membrane and transcytoplasmic openings of 1 to 3 μm. They are notably found in the liver and spleen. Discontinuous capillaries allow macromolecules to leak into the interstitium. Tumor capillaries resemble discontinuous capillaries, owing to abnormal development of wall constituents such as endothelial cell junctions, the basement membrane, and pericyte coverage (2).

Capillaries can be examined at the macroscopic level by means of CT and MRI with dynamic contrast enhancement (5). Several papers describe imaging-based quantification of the capillary microcirculation in normal organs and tumors (6, 7). Dynamic contrast enhanced (DCE) imaging can be used to calculate microcirculatory parameters such as blood flow (or tissue perfusion) and capillary permeability, based on contrast agent leakage through the endothelial wall. This leakage is dependent on the type of capillary and on the molecular size of the contrast agent, and can be used to distinguish benign from malignant tumors (8, 9). DCE imaging is also useful for monitoring the effect of antiangiogenic drugs, as changes in microvascular parameters (10) appear earlier than changes in tumor size (11). In DCE imaging, microcirculatory parameters are quantified at the macroscopic voxel level, which represents the average of a large number of capillaries. Here we attempted to visualize and quantify phenomena underlying microcirculatory parameters *in vivo*, and particularly capillary permeability, by means of microscopic DCE imaging.

Since the 1970s, intravital fluorescence microscopy has provided useful patho physiologic information on the microcirculation at the microscopic scale. However, most experimental models require a surgical procedure to expose the tissue of interest. A new fibered confocal fluorescence microscopy (FCFM) (12) device (Cell viZio™) has since been developed to study the microcirculation with minimally invasive surgery. Light from out-of-focus planes is rejected, yielding a clear image of a thin section of the target organ. Like confocal microscopy, FCFM is based on excitation of fluorescent molecules.

Here we used the Cell-viZio Device to visualize differences in the permeability of the three basic types of capillary in living mice, by using low- and high-molecular-weight contrast agents.

Materials and Methods

All experiments were performed in compliance with the national regulation for animal research.

Instrumentation

The Cell-viZio™ device (12) has three main components: a laser-based optoelectronics unit, a 1.5-mm bundle of 30 000 optical fiber mini-probes linking the scanning device to a micro lens, and software to control the system and manage video data acquisition and processing.

The laser unit provides an excitation wavelength of 488 nm and emission band wavelengths between 500 and 650 nm. The fluorescence signal is collected by the same fiber as that used for illumination. Temporal resolution of 12 frames/s can be achieved. Spatial resolution is 1.5 μm^2 in-plane, and section thickness is approximately 15 μm.

Animal Model

Healthy male Swiss nude (nu/nu) mice (Charles Rivers laboratory, L'Arbresle France) were used for mesentery and muscle capillary imaging. For tumor capillary imaging, PC3 human prostatic carcinoma cells were injected subcutaneously into both flanks of male Swiss nude mice aged 7-10 weeks and weighing 25-34 g. The mice were anesthetized by intraperitoneal injection of a 50/50 mixture of 10 ml/kg Xylazine 2% and 10 ml/kg ketamine 500 before tumor cell injection and imaging procedures.

The tumors were imaged 3 to 4 weeks after induction, when their size had reached about 5 mm.

Contrast Agents

FITC (AK Fluor 10% Akorn Millbrook, IL) and albumin FITC (Sigma, Saint Quentin Fallavier, France) were chosen because they are compatible with our imaging system (excitation 488 nm, emission 520 nm). The contrast agents were injected as a bolus into a retro-orbital vein.

FITC, a low-molecular-weight (389 daltons) contrast agent, was used at a dose of 100 μl of a 0.1 mg/ml solution (2.6×10^{-5} mmol FITC). After intravenous injection, FITC diffuses efficiently in blood and the interstitium.

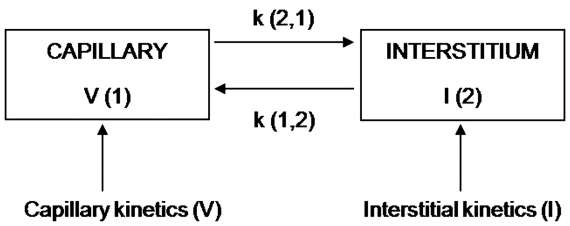

Figure 1: Drawing of Compartmental model 1. Bicompartmental model with a capillary compartment (V) and an interstitial compartment (I). The injected contrast agent enters the capillariy and, depending its molecular weight and the capillary type, diffuses into the interstitium, according to transfer constants k (2, 1) and k (1, 2).

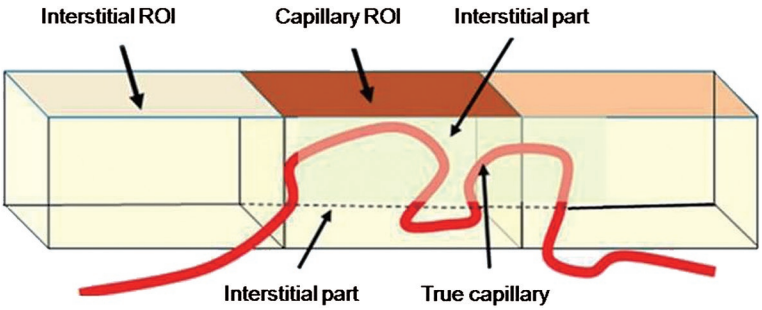

Figure 2: Voxel's drawing in fluorescence confocal microscopy. In the 3D volume observed by the fluorescence confocal microscopy, the SI measured in the capillary ROI includes an interstitial region on each side of the capillary, since the system is not strictly confocal. The SI in the solely interstitial compartment can be measured laterally to the capillary.

FITC albumin is a macromolecular agent (68,000 daltons) with efficient intravascular distribution but restricted interstitial leakage. A dose of 100 µl of a 100 mg/ml solution (140×10^{-5} mmol FITC) was injected.

In Vitro Phantom Imaging

Phantoms containing increasing concentrations of FITC and albumin FITC in water were used to determine the range of concentrations over which signal intensity was linear. To ensure reproducibility, signal intensity was controlled in these standard solutions at the end of each experiment.

In Vivo Imaging

After induction of anesthesia, the mesentery was isolated through a mid-ventral incision. Leg muscle and tumors were imaged through buttonhole incisions.

Movies were recorded continuously for 30 to 60s after contrast agent injection to observe the arrival of the bolus, then 5-s movies were recorded every minute for 10 min and for 5 min every 30 min to study capillary leakage.

The laser was turned off between each movie to avoid contrast agent bleaching and tissue heating.

Data Analysis

Raw amplitude movies were transferred to a workstation for processing with Image J software (Wayne, NIH, Bethesda, MA, USA).

The distribution and morphologic characteristics of each capillary type were assessed visually, together with the distribution and amount of capillary leakage. For quantitative measurements, a region of interest (ROI) was manually drawn in the vascular and interstitial region of each image, and was automatically propagated to all the images in the relevant series. For each new series of acquisitions, the ROIs were manually repositioned to match the coordinates of the previous series.

For the initial 30-s movie, signal intensity (SI) was measured on each image. For the following 5-s acquisitions, SI was averaged over the first five images to improve the signal-to-noise ratio.

Compartmental Models

Two models were developed to analyze the signal-intensity curves and to calculate microvascular parameters. First, we used a two-compartment model (figure 1), comprising a vascular capillary compartment (V) and an interstitial compartment (I), with bidirectional exchanges. We then used a more refined model taking into account partial volume averaging of the images, based on the compartmental model published by Wu (13). As voxel's size was larger than the capillary diameter (estimated slice thickness 15 µm, for a capillary diameter of 8 to 12 µm), the signal recorded in a ROI drawn on a capillary also included a partial volume averaging of the interstitium (figure 2). In this second model (figure 3), we considered two compartments, namely a vascular compartment (V) comprising a true vascular portion (capillary) plus an interstitial portion (I1), and a purely interstitial compartment (I2).

Signal intensities measured in the ROI were converted into concentrations by using the phantom-derived curves,

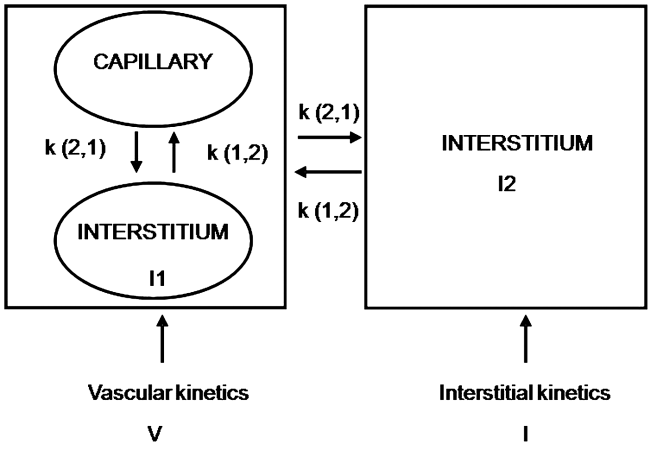

Figure 3: Drawing of Compartmental model 2 (Wu). Bicompartmental model with a vascular compartment (V), including a true vascular portion (Capillary) plus an interstitial portion (I1), and a solely interstitial compartment (I2). The contrast agent is exchanged with the vascular compartment according to the same transfer constants k (2, 1) and k (1, 2).

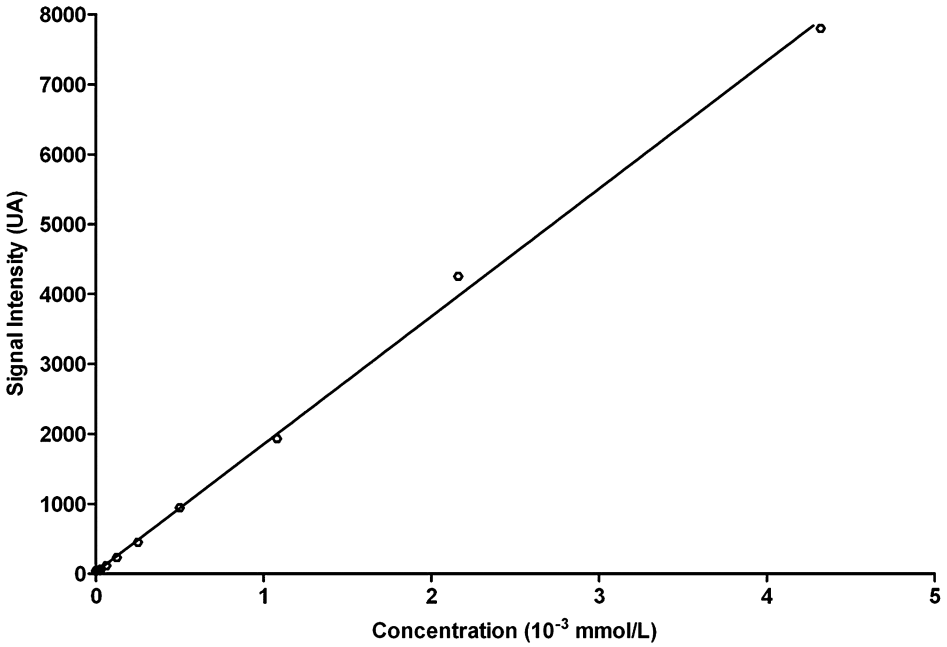

Figure 4: Graph of *in vitro* experiment with FITC. A linear relation was observed between the concentration and the signal intensity from 0 to 4.11×10^{-3} mmol/l.

thus yielding capillary (V) and interstitial kinetics (I). The two-compartment models were tested for goodness-of-fit by using SAAM I software (SAAM Institute, University of Washington, Seattle, WA, USA).

Results

In Vitro Imaging

Signal intensity was linear over a concentration range of 0 to 4.11×10^{-3} mmol/l FITC (figure 4) and 0 to 7.35×10^{-8} mmol/l albumin-FITC (figure 5).

Conversion values were the following: for FITC, SI in arbitrary units (AU) = 13 C in mmol.l; for albumin FITC, SI in AU = 27 C in mmol.l

In Vivo Imaging

Thirty-nine mice were used for video microscopy.

Five mice died, two before the beginning of the experiment, two immediately after injection (n = 2), and one after the mid-ventral incision (n = 1). The experiments lasted between 10 and 90 minutes (mean 40 minutes).

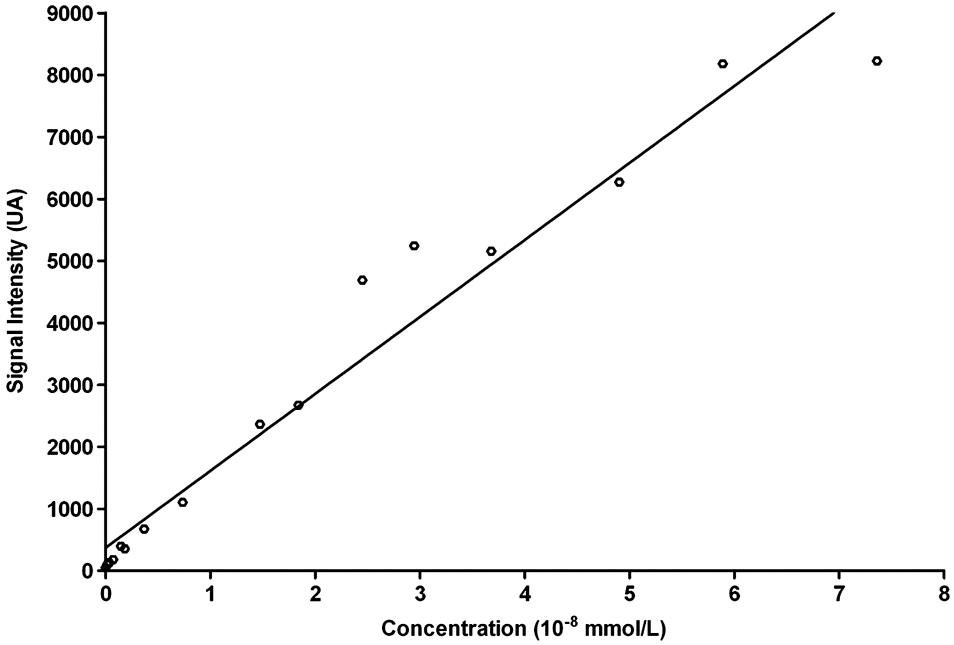

Figure 5: Graph of *in vitro* experiment with albumin FITC. A linear relation was observed between signal intensity and the macromolecule concentration from 0 to 7.35×10^{-8} mmol/l.

Table I
Summary of experiments. Number of organs correctly visualized after injection (in parentheses, number of experiments in which the first and or second passes were observed).

Contrast Agent Organ	FITC (389 daltons) (first pass observation)	Albumin FITC (68,000 daltons) (second pass observation)
Mesentery	8 (4)	10 (6)
Muscle	4 (1)	6 (4)
Tumor	2 (0)	4 (0)
Total	14	20

We studied 18 mesenteries (8 with FITC and 10 with albumin FITC), 10 leg muscles (4 with FITC and 6 with albumin FITC), and 6 tumors (2 with FITC and 4 with albumin FITC) (Table I).

Capillary Distribution and Morphology

Muscle capillaries were distributed parallel to muscle fibers and were relatively sparse (figure 6). In the mesentery, capillaries were numerous, regularly organized, and separated by fat cells (figure 7). In the tumors, the capillary network was heterogeneous (figure 8), some areas containing very few capillaries and others being hypervascularized.

Opening and closing of capillaries was clearly observed in real time, as well as changes in the direction of blood flow.

Low-Molecular-Weight Contrast Agent (FITC)

The arrival of the bolus was observed in four mesenteries and one muscle, but never in tumor capillaries. Massive interstitial leakage occurred immediately in the muscle and mesenteric sites.

The intra-capillary signal peak was observed between 7 and 13 s (mean 12 s). SI then declined gradually, reflecting renal elimination of the contrast agent. Less than 10 s after the injection, the SI increased in the interstitium mesenteric and muscle sites, likely corresponding to rapid and massive interstitial leakage (figure 9).

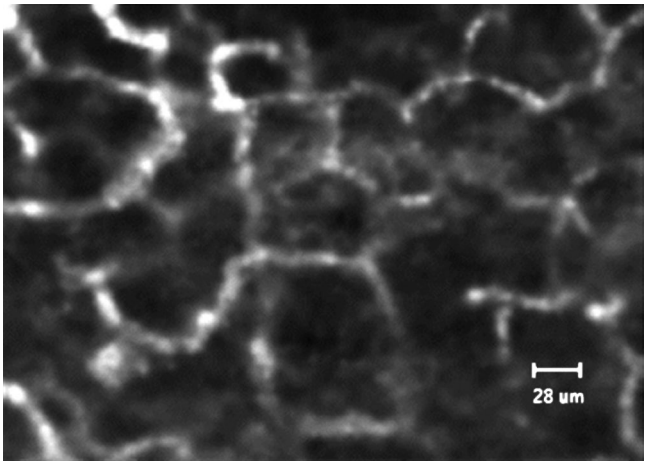

Figure 7: Picture of mesentery capillaries after albumin FITC injection. Mesentery capillaries were regular and quadrangular in shape, owing to fat-cell interposition.

No leakage was observed in tumor sites, owing to poor capillary visualization.

High-Molecular-Weight Contrast Agent (Albumin FITC)

The arrival of the bolus was observed in 6 mesenteric and 4 muscle sites, where the capillary network was very homogeneous. The contrast agent remained in the capillaries at both sites for up to 90 minutes, and no leakage was noted.

The intra-capillary signal peak occurred after 4 to 10 s (mean 6 s). It was followed by a second peak, likely corresponding to recirculation, and then by a plateau representing steady-state

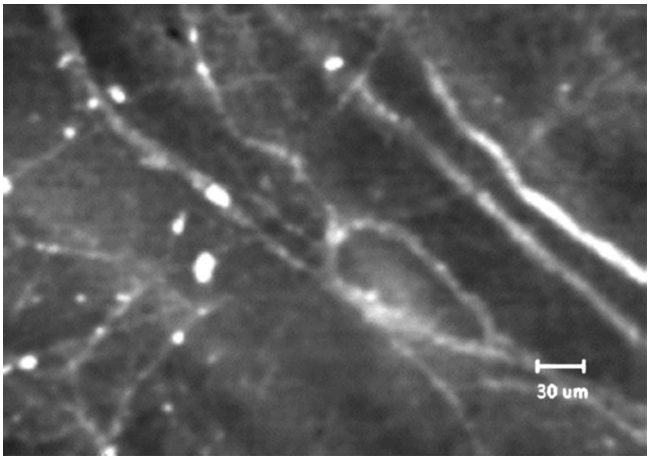

Figure 6: Picture of muscle capillaries after albumin FITC injection. The muscle capillaries were regular, linear and parallel to muscle fibers.

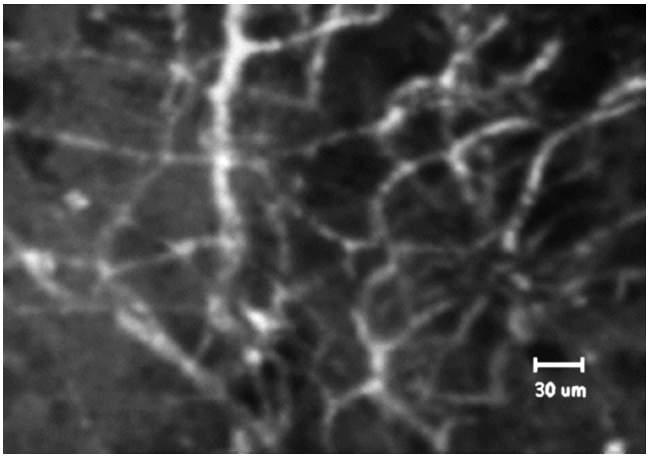

Figure 8: Picture of tumor capillaries after albumin FITC injection. Tumor capillaries were irregular and tortuous and had a heterogeneous distribution.

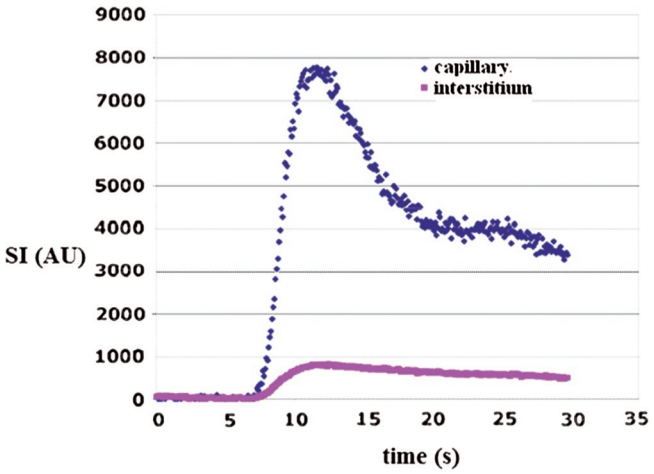

Figure 9: Graph of mesenteric capillary and interstitial enhancement after FITC injection. This figure illustrates a typical SI-time curve in a mesenteric capillary and in an interstitial area after FITC injection. The arrival of the bolus was clearly observed in the capillary, and was followed by a gradual signal decline due to contrast agent distribution. Starting 7 s after injection there was a gradual increase in the interstitial SI, corresponding to rapid leakage of the contrast agent, followed by a plateau phase.

(figure 10). There was no significant change in the interstitial SI during the 16-minute observation period, in keeping with the intravascular properties and restricted leakage of albumin FITC (figure 11) (14).

As with FITC, the arrival of the albumin FITC bolus was never observed in the tumor sites. This was due to the difficulty of finding a richly vascularized region.

Five minutes after albumin FITC injection, high signal intensity was observed in the interstitium at two tumor sites, suggesting capillary leakage. The SI then declined strongly at the capillary and interstitial sites until the end of the observation period. In a representative animal (figure 12) the SI fell by 46% in the capillary site and 60% in the interstitial site between the fifth and the sixth minutes after injection.

In another animal, the contrast agent accumulated on the capillary inner walls (figure 13).

Compartmental Models

Despite visually satisfactory experimental curves, neither compartmental model yielded microvascular parameters for any of the three types of capillary. Model 1 fitted the mesenteric FITC curves satisfactorily but the algorithm did not converge correctly and the model was unstable. We did not succeed in obtaining values for the transfer parameters k (1.2) and k (2.1). Likewise, with the more complex model 2, integrating partial voluming, no acceptable fit of the experimental curves was obtained at any site with either FITC or albumin FITC.

Discussion

Small-animal imaging modalities can be categorized by their resolution and invasiveness. Here we examined the capacity of a new FCFM device to visualize the microcirculation in living mice. This technique offers a compromise between optical probe dimension (diameter as small as 650 μm), real-time capabilities (12 frames/s), spatial resolution (2-5 μm), and confocality. DCE imaging based on US, CT or MRI can be used to study the microcirculation at the macroscopic scale (15, 16), and phenomena occurring on a microscopic level can therefore only be hypothesized.

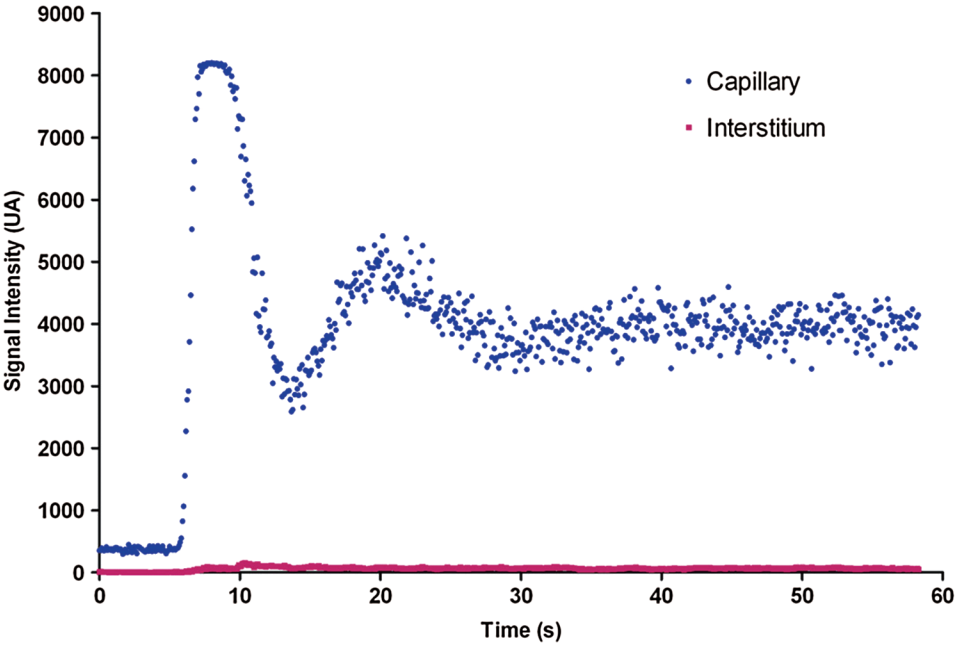

Figure 10: Graph of mesenteric capillary and interstitial enhancement after albumin FITC injection. This figure illustrates a typical SI-time curve during the first 60 seconds after albumin FITC injection, in a mesenteric capillary and interstitium. The arrival of the bolus was clearly observed, as with FITC, but a second peak was observed after 20 s, before the plateau phase, likely corresponding to the second pass of the macromolecular contrast agent.

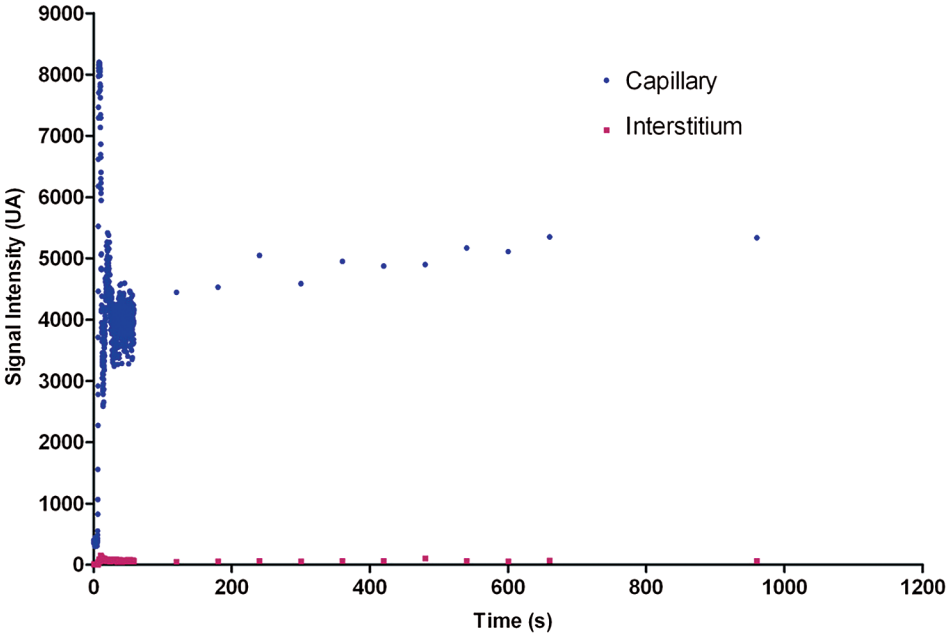

Figure 11: Graph of mesenteric capillary and interstitial enhancement over 16 minutes after albumin FITC injection. After the second peak, the capillary SI plateaued, representing steady-state. In the interstitium, the signal remained very low during the observation period, indicating no significant capillary leakage of the macromolecular agent.

We studied the morphology of three types of capillary, in muscle (continuous), the mesentery (fenestrated) and tumors (discontinuous). We successfully and reproducibly observed the arrival of the bolus of the low-molecular-weight contrast agent (FITC) and the high-molecular-weight contrast agent (albumin FITC) in muscle and the mesentery, as previously described with macroscopic DCE imaging (CT and MRI). At these two sites the capillaries were regularly distributed, and capillaries were almost always present within the image. We confirmed the solely intravascular distribution of the macromolecular contrast agent in muscle and mesenteric capillaries. In contrast, about 50% of the low-molecular-weight contrast agent leaked out from muscle and mesentery capillaries during the first pass, in keeping with previous studies (17, 18).

The arrival of the bolus was never observed at tumor sites, probably owing to technical difficulties. Indeed, the tumors were heterogeneous and contained irregular capillary networks and non vascularized areas of necrosis. Unfortunately, it was not possible to locate vascularized areas before injecting the contrast agent. We detected the macromolecular contrast agent in the interstitium of the tumors but not of the mesentery or muscle, suggesting that

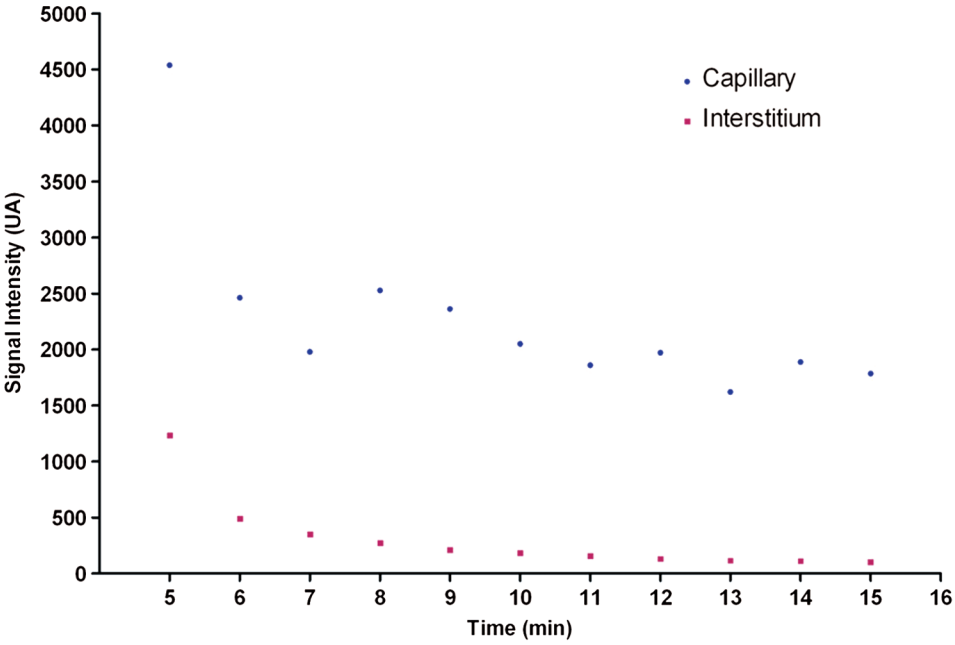

Figure 12: Graph of tumor capillary and interstitial enhancement between 5 and 16 minutes after albumin FITC injection. Kinetic studies were not possible shortly after the bolus, but 5 minutes after albumin FITC injection a high SI was observed in the interstitium, likely corresponding to capillary leakage of the macromolecular contrast agent. The SI then fell gradually both in the capillary and in the interstitium.

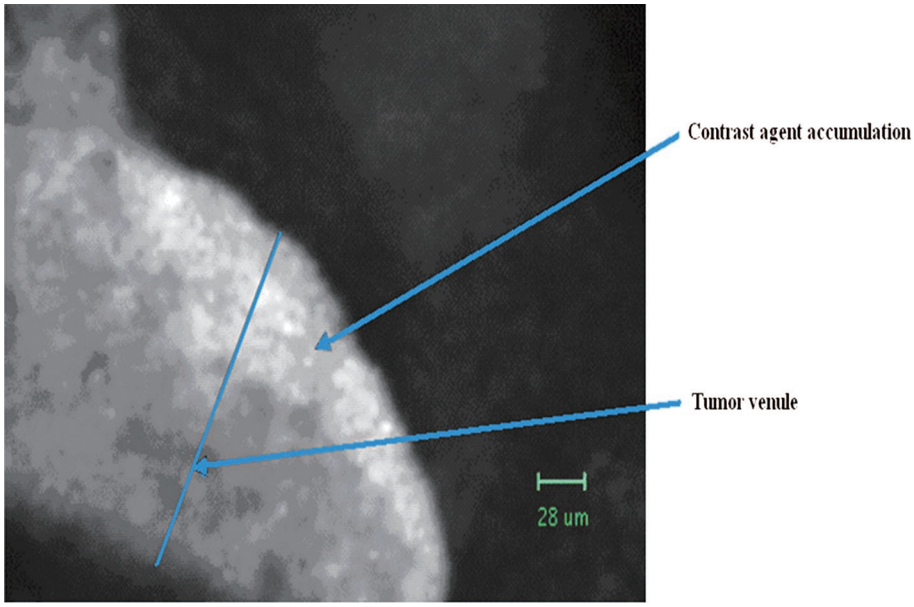

Figure 13: Picture of tumor capillary after albumin FITC injection. This picture shows a phenomenon observed only in the tumors: the macromolecular contrast agent appeared to stick to the interior capillary walls. This may have been due to tissue overheating and coagulation of the albumin-based contrast agent.

tumor capillaries are leakier, in keeping with the reported permeability of tumor capillaries due to endothelial wall defects (4). Interestingly, even though we turned the laser off between acquisitions to avoid bleaching, we observed a significant decline in the tumor SI. However, compared to normal capillaries, blood flow may be slowed by the abnormal and tortuous morphology of tumor capillaries (19). If so, fluorophore molecules would be illuminated for longer, possibly leading to bleaching. In this case, the rate of bleaching might have the potential to be used to quantify blood flow.

Despite the use of fluorophore concentrations within the range of linear signal intensities *in vitro*, and the visually satisfactory experimental curves, we were unable to quantify the microcirculation, as neither compartmental model yielded valid microvascular parameters. A satisfactory fit of the experimental curves was obtained with compartmental model 1, but the model was unstable, preventing us from obtaining quantitative values for the microvascular parameters (k (1.2) and k (2.1)). This bicompartmental model may be too simple for optical imaging. Factors potentially responsible for the failure to quantify microvascular parameters include breathing artifacts and partial voluming in the ROI. Also, in optical imaging there is a complex relation between signal intensity and the contrast agent concentration, and the relationship between signal intensity and the fluorophore concentrations used in our study may not have been linear in living tissues. In addition, when a tissue is illuminated by photons, many factors may induce signal loss. Natural tissue chromophores such as hemoglobin and collagen can absorb excitatory or emitted photons without emitting fluorescence, thus reducing the measured signal. In addition, diffusion scatters photons in several directions. Several teams have developed complex models to quantify the optical signal (20, 21).

Marked variability was observed at different sites in a given animal. The small observation window of this device makes the signal highly dependent on local heterogeneity, and the observed portion of tissue may not be representative. This is a limit of all microscopy techniques, whereas tissue heterogeneity is compensated for by averaging in macroscopic techniques as CT and MRI.

The main limit of this study is the lack of a reference method. DCE imaging provides only macroscopic information on the microcirculation, while confocal microscopy requires the use of perfused organs *ex vivo*, meaning that it may not be possible to extrapolate the results for blood flow and capillary permeability to the *in vivo* situation.

In conclusion, this study shows the feasibility of confocal fluorescence microscopy for studying the microcirculation and capillary permeability *in vivo*, but further development is required to provide quantitative data.

Conflict of Interest

No conflict of interests for all authors.

References

1. Staub, N. C. The emerging role of the microcirculation in clinical medicine. *J Lab Clin Med 98,* 311-322 (1981).
2. Hashizume, H., Baluk, P., Morikawa, S., McLean, J. W., Thurston, G., Roberge, S. Openings between defective endothelial cells explain tumor vessel leakiness. *Am J Pathol 156*, 1363-1380 (2000).
3. Bedard, N., Pierce, M., El-Nagger, A., Anandasabapathy, S., Gillenwater, A., Richards-Kortum, R. Emerging roles for multimodal

optical imaging in early cancer detection: a global challenge. *Technol Cancer Res Treat 9*, 211-217 (2010).
4. Palade, G. E. Fine structure of blood capillaries. *J Appl Physiol 24,* 1424 (1953).
5. Padhani, A. R. Dynamic contrast-enhanced MRI in clinical oncology: current status and future directions. *J Magn Reson Imaging 16*, 407-422 (2002).
6. Cuenod, C. A., Fournier, L., Balvay, D., Guinebretière, J. M. Tumor angiogenesis: pathophysiology and implications for contrast-enhanced MRI and CT assessment. *Abdom Imaging 31,* 188-93 (2006).
7. Fournier, L. S., Cuenod, C. A., de Bazelaire, C., Siauve, N., Rosty, C., Tran, P. L. Early modifications of hepatic perfusion measured by functional CT in a rat model of hepatocellular carcinoma using a blood pool contrast agent. *Eur Radiol 14*, 2125-2133 (2004).
8. D'Assignies, G., Couvelard, A., Bahrami, S., Vullierme, M. P., Hammel, P., Hentic, O. Pancreatic endocrine tumors: Tumor blood flow assessed with perfusion CT reflects angiogenesis and correlates with prognostic factors. *Radiology 250*, 407-416 (2009).
9. Roberts, H. C., Roberts, T. P., Brasch, R. C., Dillon, W. P. Quantitative measurement of microvascular permeability in human brain tumors achieved using dynamic contrast-enhanced MR Imaging: Correlation with histologic grade. *Am J Neuroradiol 21*, 891-899 (2000).
10. Fournier, L. S., Novikov, V., Lucidi, V., Fu ,Y., Miller, T., Floyd, E. MR monitoring of cyclooxygenase-2 inhibition of angiogenesis in a human breast cancer model in rats. *Radiology 243*, 105-111 (2007).
11. Pradel, C., Siauve, N., Bruneteau, G., Clement, O., de Bazelaire, C., Frouin, F. Reduced capillary perfusion and permeability in human tumour xenografts treated with the VEGF signalling inhibitor ZD4190: an in vivo assessment using dynamic MR imaging and macromolecular contrast media. *Magn Reson Imaging 21*, 845-851 (2003).
12. Laemmel, E., Genet, M., Le Goualher, G., Perchant, A., Le Gargasson, J. F., Vicaut, E. Fibered confocal fluorescence microscopy (Cell-viZio) facilitates extended imaging in the field of microcirculation. A comparison with intravital microscopy. *J Vasc Res 41,* 400-411 (2004).
13. Wu, N. Z., Klitzman, B., Rosner, G., Needham, D., Dewhirst, M. W. Measurement of material extravasation in microvascular networks using fluorescence video-microscopy. *Microvasc Res 46,* 231-253 (1993).
14. Laux, V., Seiffge, D. Mediator-induced changes in macromolecular permeability in the rat mesenteric microcirculation. *Microvasc Res 49*, 117-133 (1995).
15. Ellegala, D. B., Leong-Poi, H., Carpenter, J. E., Klibanov, A. L., Kaul, S., Shaffrey, M. E. Imaging tumor angiogenesis with contrast ultrasound and microbubbles targeted to αvβ3. *Circulation 108*, 336-341 (2003).
16. Feng, S. T., Sun, C. H., Li, Z. P., Mak, H. K., Peng, Z. P., Guo, H. Y. Evaluation of angiogenesis in colorectal carcinoma with multidetector-row CT multislice perfusion imaging. *Eur J Radiol* (2009). [Epub ahead of print]
17. Daldrup, H. E., Shames, D. M., Husseini, W., Wendland, M. F., Okuhata, Y., Brasch, R. Quantification of the extraction fraction for gadopentetate across breast cancer capillaries. *Magn Reson Med 40*, 537-543 (1998).
18. Kovar, D. A., Lewis, M. Z., River, J. N., Lipton, M. J., Karczmar, G. S. In vivo imaging of extraction fraction of low-molecular-weight MR contrast agents and perfusion rate in rodent tumors. *Magn Reson Med 38*, 259-268 (1997).
19. Carmeliet, P., Jain, R. K. Angiogenesis in cancer and other diseases. *Nature 407*, 249-257 (2000).
20. Ntziachristos, V., Schellenberger, E. A., Ripoll, J., Yessayan, D., Graves, E., Bogdanov, A., Jr. Visualization of antitumor treatment by means of fluorescence molecular tomography with an annexin V-Cy5.5 conjugate.*Proc Natl Acad Sci USA 101*, 12294-12299 (2004).
21. Cuccia, D. J., Bevilacqua, F., Durkin, A. J., Merritt, S., Tromberg, B. J., Gulsen, G. In vivo quantification of optical contrast agent dynamics in rat tumors by use of diffuse optical spectroscopy with magnetic resonance imaging coregistration. *O Appl Opt 42*, 2940-2950 (2003).

Received: XX XX, XXXX; Revised: XX XX, XXXX;
Accepted: XX XX, XXXX